

This is a preprint from the author's website www.geraldartner.com

This is the accepted version of the following article

Gerald Artner, "Improving Mobile Communications with Antennas that Map the Channel and Move to Local Maxima," *Microwave and Optical Technology Letters*, pp. 1-7, 2023, DOI: 10.1002/mop.33594, which has been published in final form at <https://doi.org/10.1002/mop.33594>. This article may be used for non-commercial purposes in accordance with the Wiley Self-Archiving Policy [<http://www.wileyauthors.com/self-archiving>].

ARTICLE TYPE

Improving Mobile Communications With Antennas That Map the Channel and Move to Local Maxima

Gerald Artner*

¹TÜV AUSTRIA Services, TÜV
AUSTRIA Group, Vienna, Austria

Correspondence

*Gerald Artner, Institute of
Telecommunications, Technische
Universität Wien, Gusshausstrasse 25
/ E389, 1040 Vienna, Austria, Email:
gerald.artner@tuwien.ac.at,
www.geraldartner.com

Summary

A technique is proposed that improves wireless communication channels in fading environments. The device creates a map of channel measurements. The device then moves its antenna to positions of the previously measured maximum within its reach. Proof-of-concept measurements were performed for smartphone-sized devices in an office environment. A quarter-wavelength monopole antenna for the 2.4 GHz frequency band successfully kept the channel at local maxima. The results show that small antenna movements over half of a wavelength are sufficient to keep the channel in local maxima, to avoid deep fading notches, and to improve channels over state-of-the-art antennas that move with their devices. A channel model for the wireless communication channel of mobile devices with channel maximum antennas is proposed based on the measurement results.

KEYWORDS:

Antenna, channel, communication, movement, vehicular, wireless

1 | INTRODUCTION

When users move their devices, they also move the antennas attached to these devices, but this movement doesn't consider the wireless channel^{1,2,3,4}. From a communication viewpoint, the antenna movements through the surrounding area are arbitrary. Consequently, when devices move in fading environments, the antenna movements and positions in the spatial fading pattern will be arbitrary and generally suboptimum. Even with multiple antenna systems that select the antenna with the best available channel or combine their signals, this wouldn't be the best channels available to the device. Devices could position their antennas accordingly, if they knew the fading pattern.

Other schemes that improve mobile communication channels with moving antennas have recently been demonstrated⁵. Antennas can perform counter-movements to stay in their original position relative to their environment and thereby keep their channels static. However, poor channels might be selected and kept static with these schemes. Consequently, antennas should move to the positions with the best channel and stay there, which this work investigates.

Several recent technical advances enable the mapping of the surrounding area and the fading pattern and real-time compensation of device movements by users. Simultaneous Localization and Mapping (SLAM) techniques⁶ have matured and are now commercially applied – most prominently in autonomous cleaning and grass cutting robots. Smartphones are equipped with Global Navigation Satellite System (GNSS) receivers, high-resolution cameras, and sensors for acceleration and tilting. Several examples highlight the possibility of real-time detection and compensation

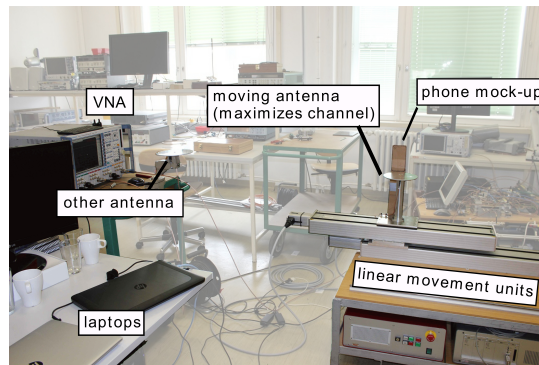


FIGURE 1 The measurement setup and the office environment.

of user-moved devices: Active suspension systems on cars⁷, stabilization of robots under outside forces^{8,9}, real-time movement compensation in walking canes¹⁰ and spoons for tremor patients¹¹. Mechanical instruments and phased arrays are highly developed to move antennas for radar applications^{12,13}, and advances in metamaterial antennas¹⁴ and reconfigurable intelligent surfaces (RIS)¹⁵ might facilitate electric movement. Mechanical antenna movement techniques for user equipment were developed for slider phones^{16,17}, but were not automated; automated movement is done, for example, in portable printers^{18,19}. Mapping of mobile communication channels, detection of device movements and appropriate antenna movements are now becoming technically feasible in real-time. Lastly, the proposed scheme is enabled by the ongoing trend toward lower wavelengths in the centimeter and millimeter region, which now fit the size of many vehicular, mobile, and portable devices.

Contribution — A technique is proposed where antennas move on devices to keep the wireless communication channel at a local maximum. The first proof-of-concept for mobile devices is conducted experimentally. It is considered that antennas perform movements within the limitations of their device’s width. Measurements were performed in an office environment with quarter-wavelength monopole antennas at 2.45 GHz. The antennas were prototyped without a mobile device and moved in a straight line for this first proof-of-concept. The data are analyzed, and a channel model is proposed for such channel maximizing antennas.

2 | EXPERIMENTAL PROOF OF CONCEPT

A proof-of-concept for channel maximizing antenna movement was demonstrated experimentally on the Vienna MIMO Testbed^{20,21}. Two quarter-wavelength monopole antennas for the 2.4 GHz Industrial, Scientific, and Medical (ISM) frequency band were placed on circular aluminum ground planes. They were connected to a vector network analyzer (VNA) to measure the channel between them in absolute value and phase. The setup was through, open, short, match (TOSM) calibrated at the antenna ports. The antennas were placed a few meters apart (120 cm at the initial position) in an office room - a typical environment for WLAN operation in the 2.4 GHz band. From a propagation viewpoint, this is a complex environment with various geometries and materials, but it’s an environment without moving objects, and the channel stays static without antenna movement. The channel maximizing antenna was mounted on two stacked high-precision linear movement units. The bottom unit moved the top unit, and a smartphone mock-up made from cardboard as a visual reference. Cardboard influence is considered to be negligible. The top unit moved the antenna. The second antenna, to which the channel was formed, remained fixed in its position. A laptop computer controlled the linear movement units and the VNA. The VNA measurements took some time, during which the antenna remained still. As a consequence, no Doppler shift²² was present in the channel. Fig. 1 shows the office environment and the experimental setup. The technical aspects and the experiment’s environment were the same as in⁵ and the results are comparable.

The movement range (device size) for the antenna to choose a channel maximum was limited to 0.5λ (about 6 cm). This is a typical width for smartphones²³. The device mock-up was moved over a distance 6λ . Photographs in Fig. 2 illustrate the principle.

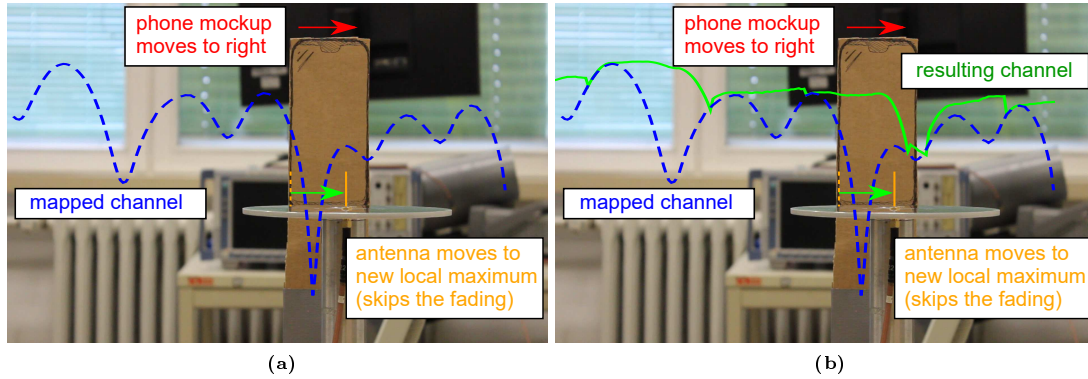


FIGURE 2 Visualization of the proposed scheme: Measured $|S_{21}|$ curves are superimposed on photos from the measurements. The antenna moves to the expected location of the local channel maximum within the phone width. a) The local maximum leaves the phone width on the left as the phone moves to the right b) The antenna moves to the new maximum position (close to the right side of the phone mockup). By doing so, it skips the deep fading notch. The communication system experiences the resulting channel (green), which no longer has deep fading notches.

TABLE 1 Pseudo-algorithm of the experiment:

```

Position  $x$  from 0 to  $6\lambda$  in  $0.02\lambda$  steps
    Move antenna to  $x$  and save channel  $C(x)$ 
End
Position  $x$  from  $0.5\lambda$  to  $6\lambda$  in  $0.02\lambda$  steps
    Move antenna to  $x_{max}$  within  $x - \lambda/2, \dots, x$ ,
    with maximum  $|S_{21}|$  of channel  $C$ .
End

```

Two measurements were performed. First, the antenna moved away from its initial position by 6λ . The channel was measured along the path and saved. Such channels are observed with antennas fixed to mobile devices and experience their small-scale fading environment as fast fading. Second, the antenna moved to local maxima within the device width of 0.5λ . The antenna selected its positions based on the first channel measurement by maximizing the scattering parameters $|S_{21}|$. Maximization of $|S_{21}|$ is a maximization of the received power and a maximization of the signal-to-noise ratio (SNR) as the noise level can be considered to be equal across the room. A pseudo-algorithm for the experiment is given in Table 1 .

3 | MEASUREMENT RESULTS

The measured $|S_{21}|$ results are shown in Fig. 3 a over the distance the device has moved from its original position. The antenna was fixed to its device like any state-of-art antenna. The channel shows small-scale fading typical in office environments due to interference of multipath components. The proposed scheme clearly shows that the channel was kept at local maxima within the device's width while it moved through the room. Communication systems with the new moving antenna wouldn't notice the fading hole, and instead, they would continuously enjoy the local channel maximum available within its reach.

The new phase in Fig. 3 b also exhibits the behavior, but the phase is not the considered metric, and therefore the positions at which it changes are arbitrary.

Fig. 3 c shows the positions of the top linear movement unit as a function of the bottom movement unit position – a visual reference of the antenna movements. In the performed experiment, the antenna starts maximizing the channel after one full device width (0.5λ). In the measurement with the regular antenna, the top movement unit stays on

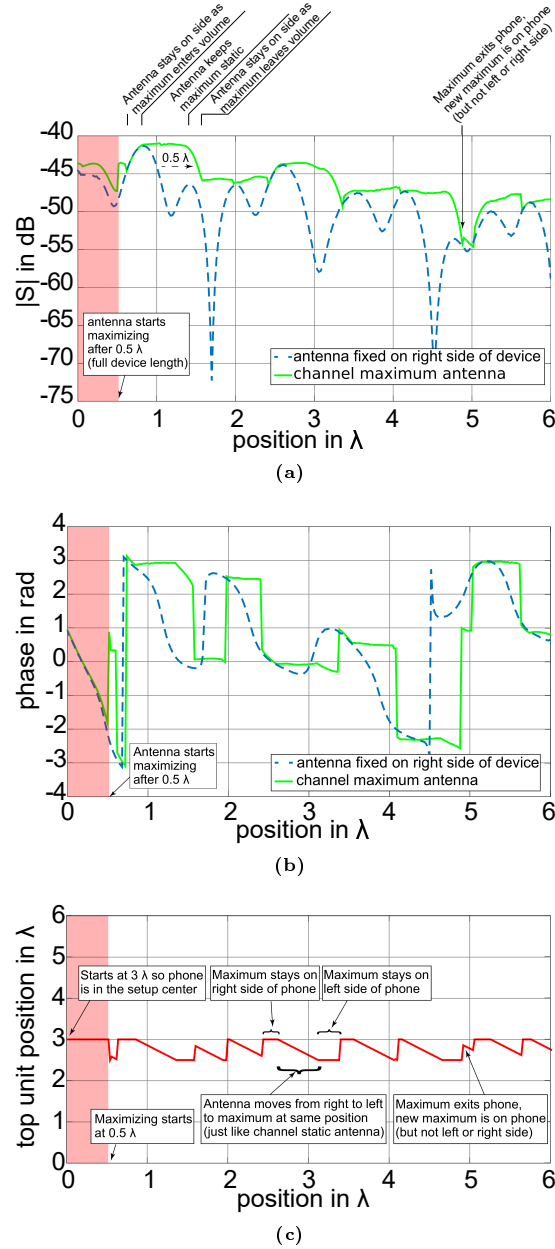


FIGURE 3 Measurement results of the channel with and without the channel maximum antenna. The antenna moves within the width of the device to maximize $|S_{21}|$. a) absolute value and b) phase. The phase is wrapped at 2π for convenient viewing. c) Positions of the top linear movement unit over positions of the bottom unit.

the right side of the volume. Typical movement patterns can be observed with the proposed scheme. Between 0.72 and 0.92λ a local maximum entered the device from the right side. The antenna stayed on the right side at the local maximum. Between 0.92 and 1.44λ the antenna performed a counter-movement opposite to the device movement to stay at the position of this maximum. From 1.44λ on, the local maximum exited the phone width towards the left side. The antenna stayed on the left side until 1.68λ where it became worse than another local maximum. The antenna moved to this local maximum and followed it until a new maximum entered on the right and so on. The regular antenna experienced a -72 dB fading hole at 1.8λ , but at the same device position, the channel maximizing antenna didn't move into the fading hole like the regular antenna did. Generally, three types of movement were observed for the channel maximizing movement:

TABLE 2 Measured mean μ (calculated as average of power), median m , maximum spread (peak-to-peak) and variances σ^2 of channel changes. The channel static antenna from⁵ was measured in the same office environment over the same 6λ distance, but at another channel realization. A theoretical comparison with perfect techniques is given on the bottom, for the plotted curves see Fig. 4 .

	power				phase		
	μ/dB	m/dB	max/dB	σ^2/dB^2	μ/rad	max/rad	σ^2/rad^2
regular (wrapped 2π)	-48.1	-49.6	30.95	23.6650	0.601	6.223	2.4992
regular (unwrapped)	-"	-"	-"	-"	-6.517	12.847	10.1141
channel max. movement (wrapped 2π)	-45.2	-46.5	13.68	7.9068	0.619	6.223	3.1356
channel max. movement (unwrapped)	-"	-"	-"	-"	-6.060	12.698	10.0561
channel static antenna ⁵	n.a.	n.a.	2.35	0.3595	n.a.	0.146	$9.89 \cdot 10^{-4}$
perfect maximizing movement	-45.5	-46.5	12.22	8.9236			
perfect antenna selection	-46.4	-47.7	13.91	10.797			
perfect diversity combining	-42.2	-43.4	15.54	11.357			

1. The antenna follows the position of the best channel while the maximum moves through the volume, i.e., it keeps the channel static at the maximum by performing a counter-movement opposite to the device movement as in⁵.
2. It stays at the border of the device where the slope of a maximum enters or leaves.
3. It moves to the position of a new maximum inside the volume in case the old maximum leaves.

The antenna moved along the maxima and only jumped to a different position when the channel was slightly better than the old one. Recall that the antenna only moved between VNA measurements in the experiment, so the result is more similar to electronic shifting than mechanical movement solutions. It might therefore be expected that the channel is a continuous function. In the experiment, this was not entirely the case. For example, at 5.7λ the channel had changed between the initial measurement and the measurement with the channel maximizing movement. The antenna then no longer changed positions at the optimum, which caused a discontinuity in the channel. Aspects of the channel that are not being maximized are of course full of discontinuities, as the phase measurements in Fig. 3 b show.

The statistical analysis of the data in Fig. 3 is given in Table 2 . The mean of the path loss is improved by 3 dB over the regular antenna. There is a tremendous reduction in the peak-to-peak spread (-17 dB) and the variance (-16 dB²) compared to regular antennas, but a channel static antenna⁵ reduces the channel variations even further. The statistics of the phase shift remain the same as with regular antennas.

4 | COMPARISON WITH OTHER SPATIAL DIVERSITY TECHNIQUES

The proposed technique is compared to other spatial diversity schemes. It is compared to a single antenna that is fixed to the device, with two antennas selection and two antennas combining techniques (such as equal-gain combining, maximum-ratio combining, or MIMO²⁴). The comparisons are computed as virtual arrays from the channel measurement of the single antenna measurement in Fig. 3 . The antennas for antenna selection and combining are assumed to be spaced by half of a wavelength, which was also the movement range in the experiment. This element spacing theoretically results in zero intra-array coupling for hypothetical isotropic antennas²⁵, which is approximately valid for practical omnidirectional antennas²⁶. It is further assumed that moving antennas will not influence their radiation characteristics, but in practice, the radiation characteristics of antennas are influenced by their device^{27,28}. The comparison assumes perfect channel knowledge and that moving or switching antennas takes no time.

A reference curve for combining techniques²⁹ is provided in Fig. 4 (cyan line), which is calculated as

$$20\log(|S_{21}|(x) + |S_{21}|(x - \lambda/2)), \quad (1)$$

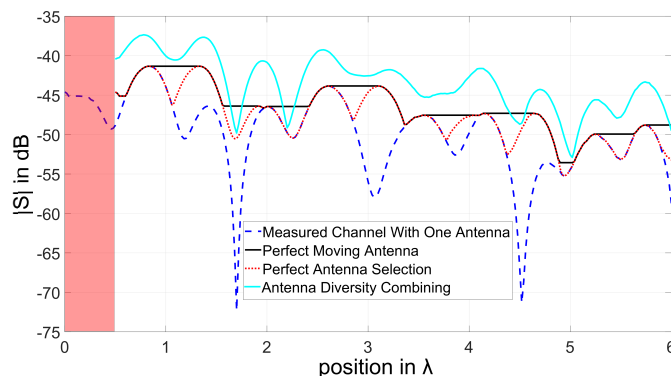


FIGURE 4 Comparison of the measured channel with a single antenna to the proposed technique, where the antenna moves to the local maximum, as well as antenna switching and signal combining. The theoretical curves are calculated as virtual arrays with antenna spacing of a range of 0.5 wavelengths.

where \log denotes the common logarithm and x is the current antenna position of the virtual array. It should be noted that techniques that combine the signals from two antennas also combine their respective noise, which is also not considered.

The virtual array comparison is given in Fig. 4 and the quantitative Table 2. A single antenna that is fixed to the device, experiences small-scale fading in its wireless communication channel as it is moved through the office environment. An antenna that can move to any position within half of a wavelength is naturally strictly better than selecting between two antennas that are spaced by half of a wavelength. Favorably, a single moving antenna will outperform signal combining techniques with two antennas when both antennas are at a local minimum of the fading pattern.

Predictor antennas that are followed by an array of static antennas have been proposed for larger objects such as cars³⁰. This could be beneficially combined with the proposed channel maximizing movement. A predictor antenna obtains a channel map, while a moving antenna positions more precisely at a maximum than interpolation between a series of fixed antennas. A direct comparison with beam-steering and pattern-reconfigurable antenna techniques³¹ is difficult. Spatial and angular resolutions of fading channels depend highly on the environment, but generally sampling two directions might give similar overall results as sampling two positions with antenna selection³². The achievable rate of advanced techniques such as interference alignment³³ and channel modulation^{34,35} also depends on the channels to the other users/antennas and channel changes are actively used. The proposed channel maximizing movement is a promising candidate for symbiosis with these schemes and not a direct competitor, seeing that these advanced schemes benefit from increased SNR and static channels.

5 | A CHANNEL MODEL FOR CHANNEL STATIC ANTENNAS

For each device position n , the antenna is moved to the position inside its available volume V . The available channel H_a is maximum according to some metric M , for example signal-to-noise ratio (SNR) or received signal strength indicator (RSSI). The channel at device position n is, therefore, the maximum channel that is available within volume V :

$$H(n) = \max_V (H_a) + N. \quad (2)$$

The model does not dispose of H_a , which can be estimated from real channels or obtained from channel models or simulations if they are spatially consistent^{36,37}. The noise term N includes channel estimation uncertainties and time-variant channel changes. Notice that the antenna and device movements are not explicitly included. Considerations that are specific to the device design, the environment or the movement are implicitly included in V and H_a . For example, the antenna might not be able to move to all positions on a device because other parts block them.

6 | CONCLUSIONS

A technique was proposed that maximizes channels by moving the antenna to mapped local maxima. The feasibility of the concept was demonstrated with an experiment in an office environment. The small-scale fading environment no longer results in a fast-fading communication channel. The scheme decreased the mean path loss by 3 dB and reduced the path loss variation (-17 dB peak-to-peak and -16 dB² variance) compared to regular antennas that move with the device.

Not every practical communication system might be able to harness the full potential of maximum channels if this means that the channel will change faster than the system can adapt. The author expects a trade-off between maximizing the channel and keeping the channel static.

ACKNOWLEDGMENTS

The author thanks Martin. Lerch of Technische Universität Wien, Vienna, Austria, for his help with the experimental work.

Financial disclosure

None reported.

Conflict of interest

The authors declare no potential conflict of interests.

References

- [1] Yoo SK, Cotton SL, Sofotasios PC, Freear S. Shadowed Fading in Indoor Off-Body Communication Channels: A Statistical Characterization Using the κ - μ /Gamma Composite Fading Model. *IEEE Transactions on Wireless Communications* 2016; 15(8): 5231–5244.
- [2] Mecklenbräuker CF, Molisch AF, Karedal J, et al. Vehicular channel characterization and its implications for wireless system design and performance. *Proceedings of the IEEE* 2011; 99(7): 1189–1212.
- [3] Artner G, Kotterman W, Del Galdo G, Hein MA. Conformal automotive roof-top antenna cavity with increased coverage to vulnerable road users. *IEEE Antennas and Wireless Propagation Letters* 2018; 17(12): 2399–2403.
- [4] Unterhuber P, Sand S, Fiebig UC, Siebler B. Path loss models for train-to-train communications in typical high speed railway environments. *IET Microwaves, Antennas & Propagation* 2018; 12(4): 492–500.
- [5] Artner G. Keeping Mobile Communication Channels Static With Antenna Counter-Movements. *IEEE Access* 2020; 8: 40088–40095.
- [6] Durrant-Whyte H, Bailey T. Simultaneous localization and mapping: part I. *IEEE Robotics & Automation Magazine* 2006; 13(2): 99–110.
- [7] Karnopp D. Active damping in road vehicle suspension systems. *Vehicle System Dynamics* 1983; 12(6): 291–311.
- [8] Brown Jr HB, Xui Y. A Single-Wheel, Gyroscopically Stabilized Robot. *IEEE Robotics & Automation Magazine* 1997.
- [9] Muehlebach M, D’Andrea R. Nonlinear analysis and control of a reaction-wheel-based 3-D inverted pendulum. *IEEE Transactions on Control Systems Technology* 2016; 25(1): 235–246.

- [10] Van Lam P, Fujimoto Y. A robotic cane for balance maintenance assistance. *IEEE Transactions on Industrial Informatics* 2019; 15(7): 3998–4009.
- [11] Pathak A, Redmond JA, Allen M, Chou KL. A noninvasive handheld assistive device to accommodate essential tremor: a pilot study. *Movement Disorders* 2014; 29(6): 838–842.
- [12] Kenyon TW. Radar antenna stabilizer. U.S. Patent 2,475,746; 1949.
- [13] Holt KJ, Vacanti DC, Pos MM. Mechanically assisted phased array for extended scan limits. U.S. Patent 10,754,020; 2020.
- [14] Jia D, He Y, Ding N, Zhou J, Du B, Zhang W. Beam-steering flat lens antenna based on multilayer gradient index metamaterials. *IEEE Antennas and Wireless Propagation Letters* 2018; 17(8): 1510–1514.
- [15] Dai L, Wang B, Wang M, et al. Reconfigurable intelligent surface-based wireless communications: Antenna design, prototyping, and experimental results. *IEEE Access* 2020; 8: 45913–45923.
- [16] Ishii J. Portable communication device. U.S. Patent 8,330,658; 2012.
- [17] Kim DH, Kim J, Choi WJ. Antenna device for portable terminal. U.S. Patent 7,532,166; 2009.
- [18] Schultz DR. Portable compact multi-function printer with cartridge paper supply. U.S. Patent 5,542,487; 1996.
- [19] Arnold GB. Portable printer and data entry device assembly. U.S. Patent 6,652,170; 2003.
- [20] Mayer M, Artner G, Hannak G, Lerch M, Guillaud M. Measurement based evaluation of interference alignment on the vienna MIMO testbed. In: VDE. ; 2013: 1–5.
- [21] Lerch M, Caban S, Mayer M, Rupp M. The Vienna MIMO Testbed: Evaluation of Future Mobile Communication Techniques. *Intel Technology Journal* 2014; 18(3).
- [22] Doppler C. *Ueber das farbige Licht der Doppelsterne und einiger anderer Gestirne des Himmels. Versuch einer das Bradley'sche Aberrations-Theorem als integrierenden Theil in sich schliessenden allgemeineren Theorie.* Königl. Böhm. Gesellschaft der Wissenschaften . 1842.
- [23] Mobile Phone & Tablet Size Comparison. <https://mobiledevicesize.com/>; . Accessed: 2021-02-07.
- [24] Hussain R, Sharawi MS. 5G MIMO Antenna Designs for Base Station and User Equipment: Some recent developments and trends. *IEEE Antennas and Propagation Magazine* 2022; 64(3): 95–107.
- [25] Ivrlač MT, Nossek JA. The multiport communication theory. *IEEE Circuits and Systems Magazine* 2014; 14(3): 27–44.
- [26] Pratschner S, Caban S, Schützenhöfer D, Lerch M, Zöchmann E, Rupp M. A fair comparison of virtual to full antenna array measurements. In: IEEE. ; 2018: 1–5.
- [27] Jesch RL. Measured vehicular antenna performance. *IEEE Transactions on Vehicular Technology* 1985; 34(2): 97–107.
- [28] Yang J, Li J, Zhou S. Study of antenna position on vehicle by using a characteristic modes theory. *IEEE Antennas and Wireless Propagation Letters* 2018; 17(7): 1132–1135.
- [29] Brennan DG. Linear diversity combining techniques. *Proceedings of the IRE* 1959; 47(6): 1075–1102.
- [30] Phan-Huy DT, Sternad M, Svensson T. Making 5G adaptive antennas work for very fast moving vehicles. *IEEE Intelligent Transportation Systems Magazine* 2015; 7(2): 71–84.
- [31] Artner G, Kowalewski J, Atuegwu J, Mecklenbräuker CF, Zwick T. Electronically steerable parasitic array radiator flush-mounted for automotive LTE. In: IEEE. ; 2019: 1–5.

- [32] Syrytsin I, Zhang S, Pedersen GF. User impact on phased and switch diversity arrays in 5G mobile terminals. *IEEE Access* 2017; 6: 1616–1623.
- [33] Yetis CM, Anand K, Kayran AH, Guan YL, Gunawan E. Implementation aspects for interference alignment. In: *IEEE*. ; 2015: 580–584.
- [34] Yildirim I, Basar E, Altunbas I. Quadrature channel modulation. *IEEE Wireless Communications Letters* 2017; 6(6): 790–793.
- [35] Mokh A, Crussiere M, H elard M, Di Renzo M. Theoretical performance of coherent and incoherent detection for zero-forcing receive antenna shift keying. *IEEE Access* 2018; 6: 39907–39916.
- [36] Pratschner S, Blazek T, Z ochmann E, et al. A spatially consistent MIMO channel model with adjustable K factor. *IEEE Access* 2019; 7: 110174–110186.
- [37] Gustafson C, Mahler K, Bolin D, Tufvesson F. The COST IRACON geometry-based stochastic channel model for vehicle-to-vehicle communication in intersections. *IEEE Transactions on Vehicular Technology* 2020; 69(3): 2365–2375.

How to cite this article: Gerald Artner (2022), Improving Mobile Communications With Antennas That Map the Channel and Move to Local Maxima, *Microw. Opt. Technol. Lett.*, 2022;xx:x–x.